Wilfredo Rosario,[1] Inderroop Singh,[1] Arnaud Wautlet,[1] Christa Patterson,[2] Jonathan Flak,[2] Thomas C. Becker,[3] Almas Ali,[1] Natalia Tamarina,[1] Louis H. Philipson,[1] Lynn W. Enquist,[4] Martin G. Myers Jr.,[2] and Christopher J. Rhodes[1]

The Brain–to–Pancreatic Islet Neuronal Map Reveals Differential Glucose Regulation From Distinct Hypothalamic Regions

ISLET STUDIES

The brain influences glucose homeostasis, partly by supplemental control over insulin and glucagon secretion. Without this central regulation, diabetes and its complications can ensue. Yet, the neuronal network linking to pancreatic islets has never been fully mapped. Here, we refine this map using pseudorabies virus (PRV) retrograde tracing, indicating that the pancreatic islets are innervated by efferent circuits that emanate from the hypothalamus. We found that the hypothalamic arcuate nucleus (ARC), ventromedial nucleus (VMN), and lateral hypothalamic area (LHA) significantly overlap PRV and the physiological glucose-sensing enzyme glucokinase. Then, experimentally lowering glucose sensing, specifically in the ARC, resulted in glucose intolerance due to deficient insulin secretion and no significant effect in the VMN, but in the LHA it resulted in a lowering of the glucose threshold that improved glucose tolerance and/or improved insulin sensitivity, with an exaggerated counter-regulatory response for glucagon secretion. No significant effect on insulin sensitivity or metabolic homeostasis was noted. Thus, these data reveal novel direct neuronal effects on pancreatic islets and also render a functional validation of the brain-to-islet neuronal map. They also demonstrate that distinct regions of the hypothalamus differentially control insulin and glucagon secretion, potentially in partnership to help maintain glucose homeostasis and guard against hypoglycemia.

Pancreatic islet α- and β-cells play a key role in regulating glucose homeostasis via controlled release of glucagon and insulin, respectively (1,2). The importance of this is indicated by the loss of pancreatic β-cell mass and/or function, resulting in glucose dysregulation and the onset of diabetes. However, the brain also mediates the control of metabolic homeostasis (3,4). A functional relationship between the brain and glucose homeostasis has been known for >160 years since Claude Bernard's "piqûre diabétique," where mechanical stimulation of the brain stem at the base of the fourth ventricle resulted in increased glycosuria (5). Later, this was found to be due to decreased insulin and increased glucagon levels mediated by direct sympathetic nerve stimulation (6). Parasympathetic stimulation of the vagus results in muscarinic-dependent stimulation of insulin secretion and muscarinic-independent glucagon secretion (7). Complementary evidence indicates that truncal vagotomy inhibits the potentiation of glucose-induced insulin secretion (8), decreases the response to insulin-induced hypoglycemia (9), and impairs the incretin secretory response of pancreatic islets (10). As such, the brain influences glucose homeostasis, in part by supplementary control of insulin and glucagon secretion via pancreatic islet innervation.

The majority of pancreatic neurons are targeted to islets in mammals, including humans (11–13). Although a recent microscopy analysis has suggested that, unlike

rodent islets, autonomic nerve endings penetrate human islets preferentially to contact the islet microcirculation (14), multiple studies have indicated a consensus that the autonomic control of islet α- and β-cell in mammals and humans is similar (15). The sympathetic effect on β-cells is mostly mediated by norepinephrine via α2 receptors, via both G_i-dependent and independent mechanisms (16,17), whereas the parasympathetic effect on β-cells is mediated by acetylcholine via M3 acetylcholine receptors and G_q-dependent mechanisms (18). Compensatory β-cell growth to insulin-resistant states may also be mediated via the brain (19,20).

Despite evidence implicating the brain's role in pancreatic islet physiology (21), the regions of the brain that communicate to pancreatic islets have not been fully defined. Pioneering studies using native pseudorabies virus (PRV) retrograde tracking of efferent neurons to the pancreas have identified certain regions of the brain stem, the midbrain, and several hypothalamic areas in this network (22,23). This is consistent with observations that lesions to the ventromedial nucleus (VMN) and paraventricular nucleus (PVN) affect the control of insulin and glucagon secretion (24). But the map of the brain-to-islet neuronal circuit has remained incomplete. Here, using a newer generation of modified attenuated PRVs that express markers to markedly improve the sensitivity and specificity for retrograde neuronal tracing, a more complete brain-to-islet neuronal network map has been generated. An initial functional validation of this map, by stereotaxic manipulation of glucose sensing in specific regions of the hypothalamus, indicated distinct effects on insulin and glucagon secretion. This underlines the regional complexity of direct central nervous system (CNS) control of pancreatic islet function, and also reveals potential novel insight into central glucose regulation of pancreatic endocrine cell function.

RESEARCH DESIGN AND METHODS

Animals
For PRV-BaBlu tracing, male and female C57BL6/J mice (16–18 weeks of age) were used. A subset of PRV-BaBlu mice were intraperitoneally injected with 2 g/kg glucose, or with saline as a control, 1 h before harvesting brains for cFos expression analysis. For PRV-Ba2001 tracing MIP-Cre[ERT] mice (C57BL6/J background strain, 16–18 weeks of age) were used, where nuclear Cre expression is specifically restricted to pancreatic β-cells when induced by tamoxifen treatment (25). Five days prior to pancreatic PRV infection of MIP-Cre[ERT] mice, tamoxifen treatment (3 × 6 mg over a course of 5 days) was administered by oral gavage to activate Cre-recombinase activity specifically in β-cells, with control animals getting an equivalent volume of water vehicle (25). Nuclear Cre-recombinase expression in β-cells of tamoxifen-treated MIP-Cre[ERT] mice was confirmed by immunofluorescent analysis of pancreatic sections, as described previously (26) (Supplementary Fig. 1). All procedures were performed under protocols approved by the University of Chicago Institutional

Animal Care and Use Committee and the University of Michigan Unit for Laboratory Animal Medicine.

Immunohistochemical Analysis
Thin sections (5–10 μm) from mouse brain or pancreas were obtained and analyzed by immunofluorescent microscopy, as described previously (26). Every fifth section was analyzed with anti–β-galactosidase (β-gal) for the PRV-BaBlu map. PRV-Ba2001 was analyzed by anti-green fluorescent protein (GFP). Stereotaxic injections were verified by anti-fLuc or anti-HKI. Secondary antibodies were from Jackson ImmunoResearch (West Grove, PA). The primary antibodies used were as follows: β-gal and GFP (Abcam, Cambridge, MA); Cre-recombinase (Novagen/Millipore, Billerica, MA); insulin (Linco/Millipore, Billerica, MA); glucokinase (GK) (Santa Cruz Biotechnology, Dallas, TX); firefly luciferase (Thermo Fisher Scientific, Bannockburn, IL), and hexokinase-1 (HK1) (Cell Signaling, Danvers, MA). For all primary antibodies, immunofluorescent analysis with controls was conducted on adjacent brain sections for autofluorescence, secondary antibody alone, and non-immune antibody preparations for the appropriate species. Anatomical brain areas were defined by the atlas of Franklin and Paxinos (27) using DAPI-positive nuclei and hematoxylin-eosin staining from adjacent sections. An average of at least 140 brain sections/animal were assessed from four or more animals.

PRV Neuronal Tracing
PRV recombinants were prepared, amplified, and purified, as described previously (28). A total of 10 μL of PRV-BaBlu or PRV-Ba2001 vector (10^8 plaque-forming units [pfu]/mL) was injected in 3- to 4-μL aliquots into three separate sites in the head, body, and tail regions of a mouse pancreas by intra-abdominal surgery. Animals were sacrificed between 24 and 120 h postsurgery as indicated, and brains were harvested, fixed in 4% (v/v) paraformaldehyde, and embedded in paraffin. Then, a series of 5- to 10-μm sections was cut, and every fifth section was analyzed by immunofluorescence and confocal microscopy, as described previously (26).

Stereotaxic-Guided Adenoviral Vector Delivery
Recombinant adenoviral (AdV) vectors were prepared, as described previously (29). Normal 12-week-old male and female C57BL6/J mice were grouped into arcuate nucleus (ARC)–, VMN-, and lateral hypothalamic area (LHA)–targeted groups ($n \geq 8$ each), and 200 nL of an AdV vector (2×10^{12} pfu/mL) was delivered specifically to the ARC, VMN, or LHA at a rate of 20 nL/min by bilateral stereotaxic-guided surgery, as described previously (30). Hypothalamic stereotaxic coordinates were obtained from the Franklin and Paxinos atlas, *The Mouse Brain in Stereotaxic Coordinates* (27), as follows: ARC −1.800 mm from bregma, ±0.295 mm mediolateral from bregma, −5.750 mm dorsoventral from bregma; VMN −1.900 mm from bregma, ±0.375 mm mediolateral from bregma, −5.550 mm dorsoventral from bregma; and LHA −1.900 mm from bregma, ±0.900 mm mediolateral from bregma, −5.500 mm dorsoventral

from bregma. As an additional "sham control," another cohort was likewise stereotaxically injected with NaCl (0.9% w/v; $n \geq 8$ for each target). All animals were allowed at least an 8-day recovery period before analyses were performed. AdV stereotaxic targeting was confirmed by immunofluorescent microscopy (26) (Supplementary Fig. 3).

Glucose and Insulin Tolerance Tests

Glucose tolerance tests (GTTs) and insulin tolerance tests (ITTs) were conducted as described previously (26). For the GTT, mice were fasted for 16 h overnight and then given an intraperitoneal dose of glucose (1 mg/g body wt). For the ITT, mice were fasted for 4 h and then given an intraperitoneal dose of insulin (0.5 mU/g body wt). Circulating insulin or glucagon levels during the GTT or ITT, respectively, were measured by ELISA (ALPCO, Salem, NH).

Metabolic Cage Analysis

Energy intake and expenditure, as well as home-cage activity and feeding and drinking behavior were studied in all animals by using a combined indirect calorimetry system (TSE Systems, Bad Homburg, Germany). After a housing adaptation of >48 h, O_2 consumption and CO_2 production were measured every 9 min for a total of 96–120 h to determine the respiratory exchange ratio and energy expenditure. Water intake and meal patterns were determined continuously, as was locomotor activity using an infrared light beam system on a x-y axis expressed as the number of beam breaks. Data from the final 48 h were accepted for analysis.

Statistical Analysis

Data are expressed as the mean $\pm$ SE of at least eight independent experiments. Results were analyzed by either ANOVA or Student t test, as appropriate, with Bonferroni post hoc corrections. A P value of ≤ 0.05 was considered to be statistically significant.

RESULTS

PRV Retrograde Tracing Reveals an Efferent Brain-to-Islet Circuit

Attenuated PRV strains specifically spread from presynaptic to postsynaptic neurons retrogradely and can traverse synapses, allowing selective in vivo tracing of efferent neurons from the brain to peripheral tissues. Newer attenuated PRV recombinants express reporter proteins, such as β-gal (PRV-BaBlu) or GFP (PRV-Ba2001), making the tracing of specific neuronal networks more facile and sensitive (28,31) than was previously possible (22,23). Initially, PRV-BaBlu (10^8 pfu/mL) was injected into normal mouse pancreata, then brains were harvested at 24, 48, 72, and 96 h postsurgery. As the majority of neuronal projections in the pancreas are targeted to pancreatic islets (13,14), it has been assumed that this approach predominantly highlights efferent brain linkage to the endocrine pancreas compared with the exocrine tissue (22,23). At 24 h, β-gal was found mostly in the brain stem nucleus tractus solitarius (NTS) and the neighboring dorsal motor nucleus of the vagus

(DMX) (Fig. 1A). Other than weak expression in the brain stem reticular formation (RF), β-gal was not detected anywhere else in the brain at this time point (Fig. 1A). At 48 h, the PRV-BaBlu β-gal was again found in the NTS and DMX, but infection had spread to the ventral brain stem, particularly the raphe (magnus, pallidus, and obscurus), the A5/C1 cell groups in the pons, the periaqueductal gray (PAG) ventral zone in the midbrain, and the Purkinje cell layer of the cerebellum (Fig. 1B). At 72 h, PRV-BaBlu β-gal appeared in the hypothalamus, most notably in the PVN, the LHA (particularly lateral/inferior to the fornix), and the ARC, with some weaker expression in the VMN and medial habenula (MeHab) of the thalamus (Fig. 2). At 96 h, β-gal was further enriched in the PVN, ARC, VMN, and LHA (Fig. 3). There was also an indication of PRV-BaBlu in the dorsomedial nucleus and the suprachiasmatic nucleus (SCN) (data not shown), as well as some indication in the limbic central amygdalar nucleus (CeA) (Fig. 3). β-Gal was not detected anywhere else in the brain or in tissues near the pancreas, such as the liver.

However, in order to further define specificity toward pancreatic islets, a PRV recombinant capable of Cre-conditional replication was used (32). PRV-Ba2001 expresses a Cre-inducible GFP reporter and the thymidine kinase enzyme. This recombinant will replicate only in cells that express Cre and, after Cre recombination, will spread to neurons that innervate the Cre-expressing cell, even if they do not express Cre. Therefore, PRV-Ba2001 GFP expression and replication can proceed only upon Cre activation, and migrate retrogradely from innervated cells into the efferent neurons that innervate them and then ascend transsynaptically to the brain. PRV tracking was conducted in MIP-Cre^{ERT} mice, where Cre is expressed only in pancreatic β-cells and Cre-driven recombination can proceed only with tamoxifen treatment causing nuclear translocation of Cre to the nucleus (25,33) (Supplementary Fig. 1). The PRV-Ba2001 recombinant (10^8 pfu/mL) was injected into pancreata of tamoxifen-treated, and vehicle-treated control, MIP-Cre^{ERT} mice. Because the PRV-Ba2001 recombinant replicates only in the Cre-expressing β-cells in MIP-Cre^{ERT} mice, fewer neurons become infected relative to PRV-BaBlu. Accordingly, brains of tamoxifen-treated and vehicle-treated control PRV-Ba2001-infected MIP-Cre^{ERT} mice were harvested after 120 h to allow for stronger labeling of neurons. A similar brain-to-islet neuronal network map was highlighted by GFP expression from the PRV-Ba2001 recombinant in tamoxifen-treated MIP-Cre^{ERT} mice (Fig. 4A), as was found after tracing with PRV-BaBlu (Figs. 1–3). The exception was that no GFP expression was observed in the cerebellum, SCN, and MeHab. No GFP expression was detected in brains of PRV-Ba2001-infected, vehicle-treated control MIP-Cre^{ERT} mice, indicating that viral replication and GFP expression were completely dependent on nuclear Cre expression (Fig. 4B). Collectively, these retrograde PRV tracing data indicate a brain-to-islet neuronal map where the main route emanates in the ARC, VMN,
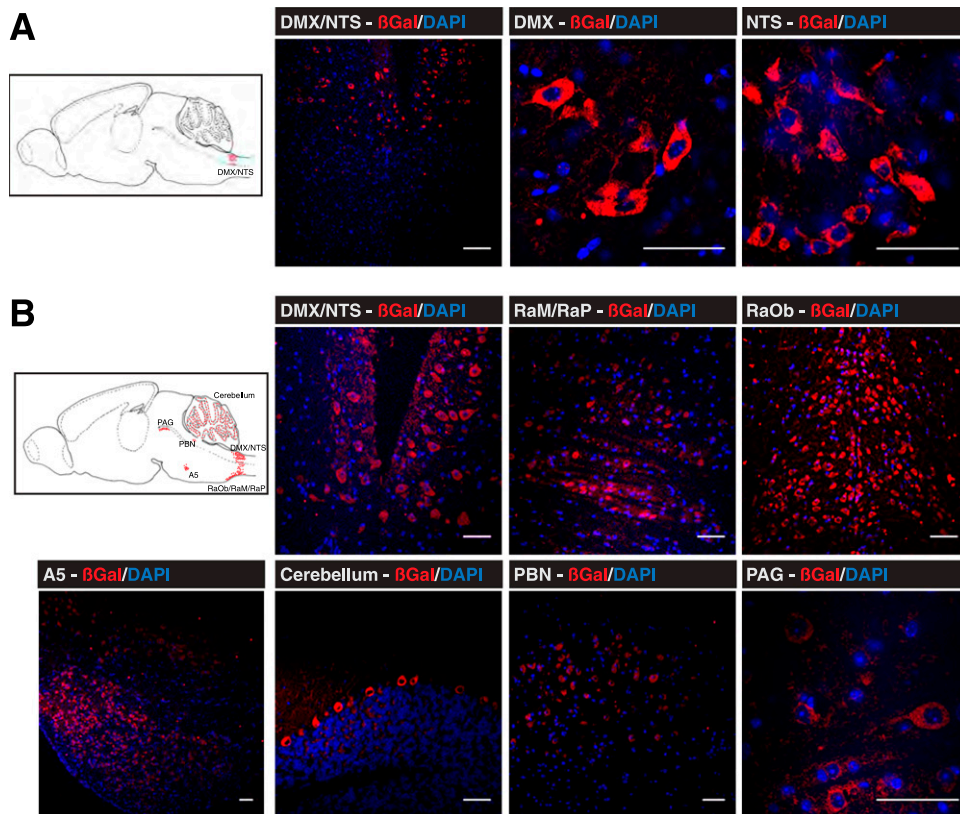
Figure 1—Brain PRV-BaBlu tracing 24 and 48 h after pancreatic infection. Mice pancreata were infected with PRV-BaBlu, and brains were subsequently analyzed for PRV-BaBlu retrograde neuronal migration, as described in RESEARCH DESIGN AND METHODS. *A*: At 24 h, β-gal expression (red) derived from PRV-BaBlu was present in brain stem neuronal cells of the NTS and DMX. *B*: At 48 h, β-gal expression (red) derived from PRV-BaBlu was present in the brain stem NTS, DMX, RaP, RaM, and RaOb regions as well as in the PBN, cerebellum, PAG, and A5 neuronal cell groups. A sagittal cartoon of the mouse brain to orient these regions is shown in each panel together with example images. The presented micrographs are from coronal sections. DAPI nuclear staining of neuronal cells is in blue. Scale bars, 50 μm. PBN, parabrachial nucleus; RaP, raphe pallidus; RaM, raphe magnus; RaOb, raphe obscurus.

and/or LHA of the hypothalamus that links through the PVN and via the PAG, or possibly via the A5 and RF regions, to then communicate with the NTS and DMX in the brain stem and onto pancreatic islets via the vagus and/or spinal cord (Fig. 4*C*).

Colocalization of Hypothalamic GK Within the Brain-to-Islet Neuronal Map

GK is a key enzyme for sensing glucose in the physiological range, and is exclusively expressed in pancreatic α- and β-cells, certain gut cells, some hypothalamic neurons, and the liver. Separate tissue-specific promoter activity on the GK gene yields liver and β-cell (GK$_\beta$) isoforms, and it is the latter that is expressed in the hypothalamic neuron (34,35). The brain-to-islet neuronal map was examined for GK$_\beta$-expressing neurons coexpressed with β-gal in brain sections of mice whose pancreata were infected with PRV-BaBlu 96 h previously (Fig. 3). Areas that showed significantly higher β-gal/GK$_\beta$ colocalization were the ARC, VMN, and LHA hypothalamic nuclei relative to certain other regions highlighted in the brain-to-islet neuronal map by PRV-BaBlu (Fig. 5*A* and *B*). This suggested a role for glucose sensing within these three hypothalamic nuclei that, in turn, could influence the efferent projections linking to

pancreatic islet cells. Glucose activation of CNS neurons was probed by induced cFos expression in some of the PRV-BaBlu pancreas–infected mice. Immediately adjacent serial sections (5 μmol/L) were then assessed for β-gal/GK and β-gal/cFos expression, and several β-gal/GK/cFos–coexpressing neurons were observed in hypothalamic regions of the glucose-treated mice, particularly in the ARC. As such, GK-expressing neurons within the brain-to-islet can be activated by glucose (Supplementary Fig. 2).

Functional Validation of the Brain-to-Islet Neuronal Map

Hypothalamic Glucose Sensing in GTTs

In order to examine whether the brain-to-islet neuronal map has functional relevance in direct control of pancreatic islet α- and/or β-cell function, the three hypothalamic nuclei that indicated the most GK$_\beta$ expression (Fig. 5), and likely have glucose-sensing activity within the brain-to-islet neuronal map (Fig. 4*C*), were targeted. The mechanism and molecular components of glucose sensing in certain hypothalamic neuronal cells are not nearly as well defined as they are in pancreatic β-cells (21,36). Indeed, some GK$_\beta$-expressing neuronal cells may sense glucose by
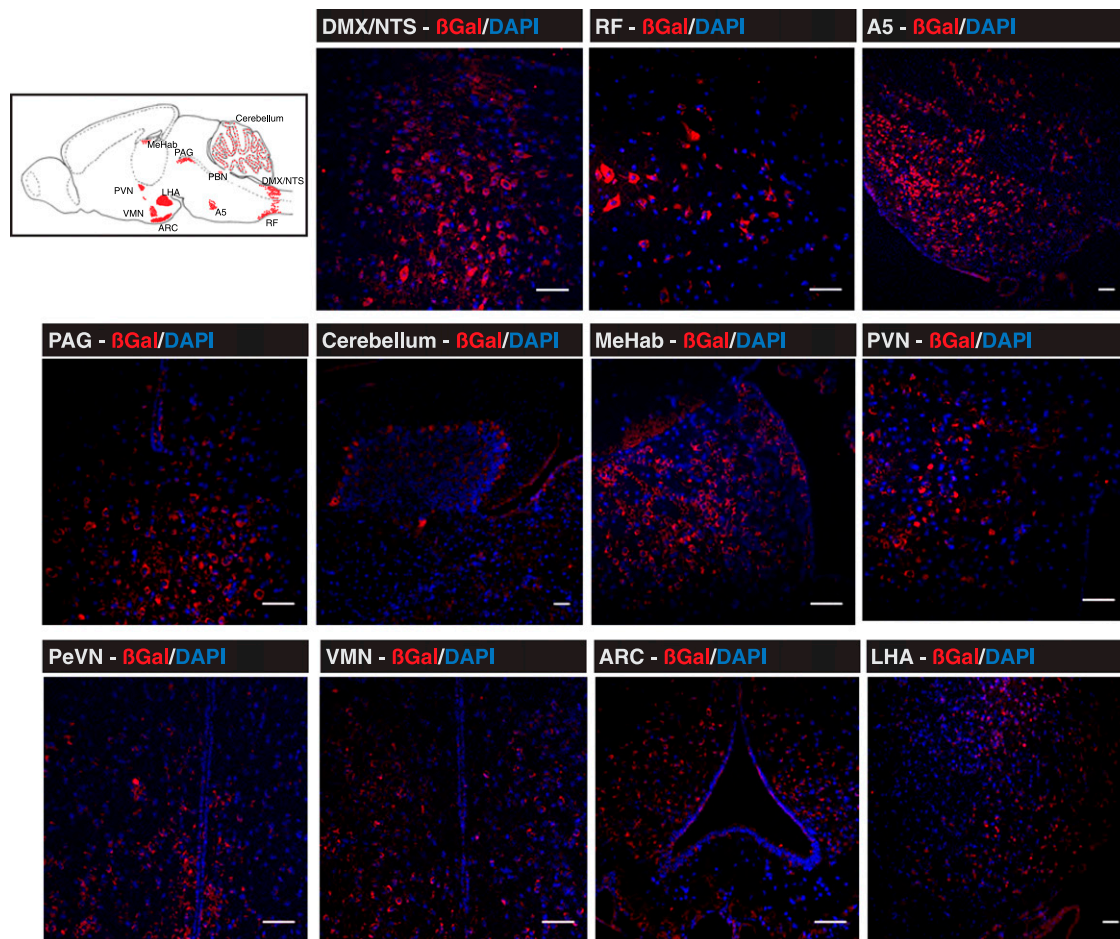
Figure 2—Brain PRV-BaBlu tracing 72 h after pancreatic infection. Mice pancreata were infected with PRV-BaBlu, and brains were subsequently analyzed for PRV-BaBlu retrograde neuronal migration, as described in RESEARCH DESIGN AND METHODS. At 72 h, β-gal expression (red) derived from PRV-BaBlu was present in brain stem neuronal cells of the NTS, DMX, and RF regions; the PAG, cerebellum, and A5 regions; the MeHab in the thalamus; and the PVN, periventricular nucleus (PeVN), VMN, ARC, and LHA regions of the hypothalamus. A sagittal cartoon of the mouse brain to orient these regions is shown together with example images. The presented micrographs are from coronal sections. DAPI nuclear staining of neuronal cells is in blue. Scale bars, 50 μm.

different mechanisms (21). In pancreatic β-cells, glucose sensing in the physiological range is governed mostly by a combination of facilitated glucose transport by GLUT2 and GK, which have a K_m for glucose in the appropriate millimolar range (36). But this is on top of ubiquitously expressed GLUT1 and HK1 that have a K_m for glucose in the micromolar range (37). Thus, it is the GK/HK1 ratio activity that is key to β-cell glucose sensing, trapping glucose in the cell to generate metabolic signals that are relative to its circulating concentrations (36,37). It is quite unclear whether a similar mechanism of glucose sensing applies to GK_β-expressing neuronal cells. However, analogous to β-cells, it is possible that artificially increased HK1 expression could interfere with glucose sensing specifically in GK_β-expressing neuronal cells. To test whether glucose sensing in the ARC, VMN, and/or LHA can have a direct effect on pancreatic islet physiology, a stereotaxic approach was used to deliver an AdV vector expressing HK1 specifically to each of these hypothalamic regions in mice. Increasing the expression of HK1 relative to endogenous GK_β may effectively left-shift glucose-sensing activity toward the micromolar range as it does in β-cells, enabling the affected cells to sense glucose at lower levels relative to the circulating glucose levels (38). Increased expression of HK1 in non–GK–expressing cells would not be expected to have much of a consequence for altering the threshold for glucose sensing because the K_m for glucose would be unaltered (37). An AdV expressing firefly luciferase (AdV-fLuc) and sham saline injections were used as controls. Stereotaxic injection site–specific targeting was confirmed by immunofluorescence (Supplementary Fig. 2). As previously defined, there is little spread of AdV-mediated expression away from the injection site, so this approach is quite specific to the regions targeted (39). It must be emphasized that this manipulation was primarily designed to see whether the same manipulation in different regions of the hypothalamus had any differential effect on islet cell
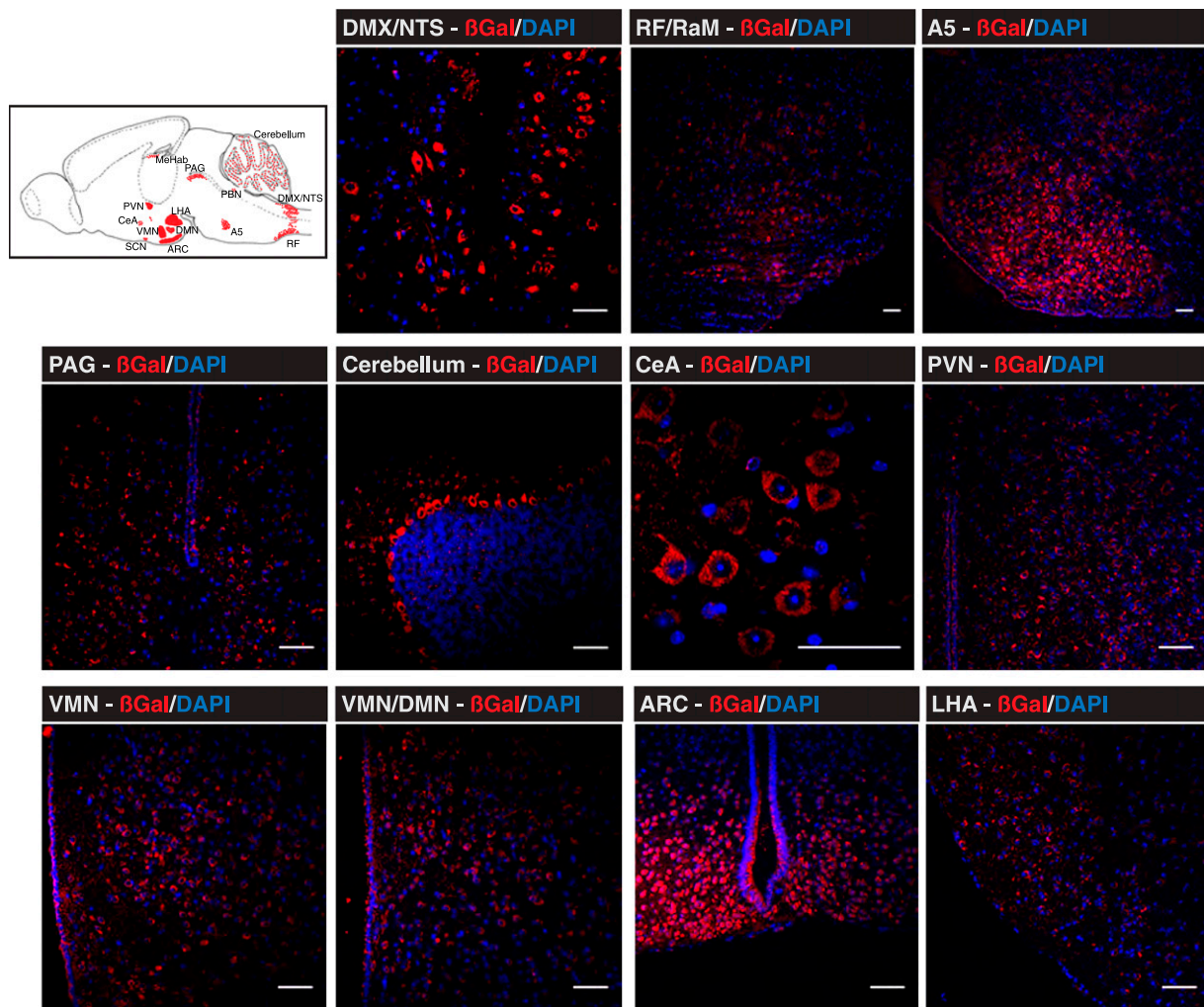
Figure 3—Brain PRV-BaBlu tracing 96 h after pancreatic infection. Mice pancreata were infected with PRV-BaBlu, and then brains were subsequently analyzed for PRV-BaBlu retrograde neuronal migration, as described in RESEARCH DESIGN AND METHODS. At 96 h, β-gal expression (red) derived from PRV-BaBlu was further concentrated in brain stem neuronal cells of the NTS, DMX, and RF regions; the PAG, cerebellum, and A5 regions; and the PVN, VMN, ARC, and LHA regions of the hypothalamus. It was also detectable in the CeA. A sagittal cartoon of the mouse brain to orient these regions is shown together with example images. The presented micrographs are from coronal sections. DAPI nuclear staining of neuronal cells is in blue. Scale bars, 50 μm. DMN, dorsomedial nucleus; PBN, parabrachial nucleus; RaM, raphe magnus.

functions to help validate the brain-to-islet neuronal map. Whether this has relevance to hypothalamic control of glucose homeostasis was considered secondarily.

Mice with ARC-targeted HK1 overexpression had increased fasting blood glucose levels relative to AdV-fLuc and sham-treated control animals ($P \leq 0.05$) (Fig. 6B), and were glucose intolerant when subjected to a GTT ($P \leq 0.05$) (Fig. 6A and C). This was due to an ~50% decrease in glucose-induced insulin secretion during the GTT ($P \leq 0.05$) (Fig. 6D and F). Fasting insulin levels were unchanged relative to those of control animals (Fig. 6E). Mice with VMN-targeted HK1 overexpression showed normal glucose homeostasis relative to AdV-fLuc and sham control mice (Fig. 6G–I), although insulin secretion during the GTT was reduced by ~25% ($P \leq 0.05$) (Fig. 6J and L). In contrast, mice with LHA-targeted HK1 overexpression had significantly decreased overnight fasting blood glucose levels relative to those of AdV-fLuc and sham control animals ($P \leq 0.05$) (Fig. 6O), and significantly improved glucose tolerance in the GTT ($P \leq 0.05$) (Fig. 6M and N). However, there was no change in fasting insulin levels (Fig. 6Q) or in vivo insulin secretion during the GTT relative to control animals (Fig. 6P and R).

Hypothalamic Glucose Sensing in ITTs
ITTs were also conducted in the mice overexpressing HK1 in the ARC, VMN, or LHA in comparison with fLuc-expressing and sham control mice to examine the counter-regulatory response to hypoglycemia and reactive glucagon secretion. Mice with ARC-targeted HK1 overexpression showed no indication of a change in insulin sensitivity, as judged by the initial (0–60 min) downward decrease in glucose levels on the ITT, relative to control animals (Fig. 7A). Neither was there any significant difference in a
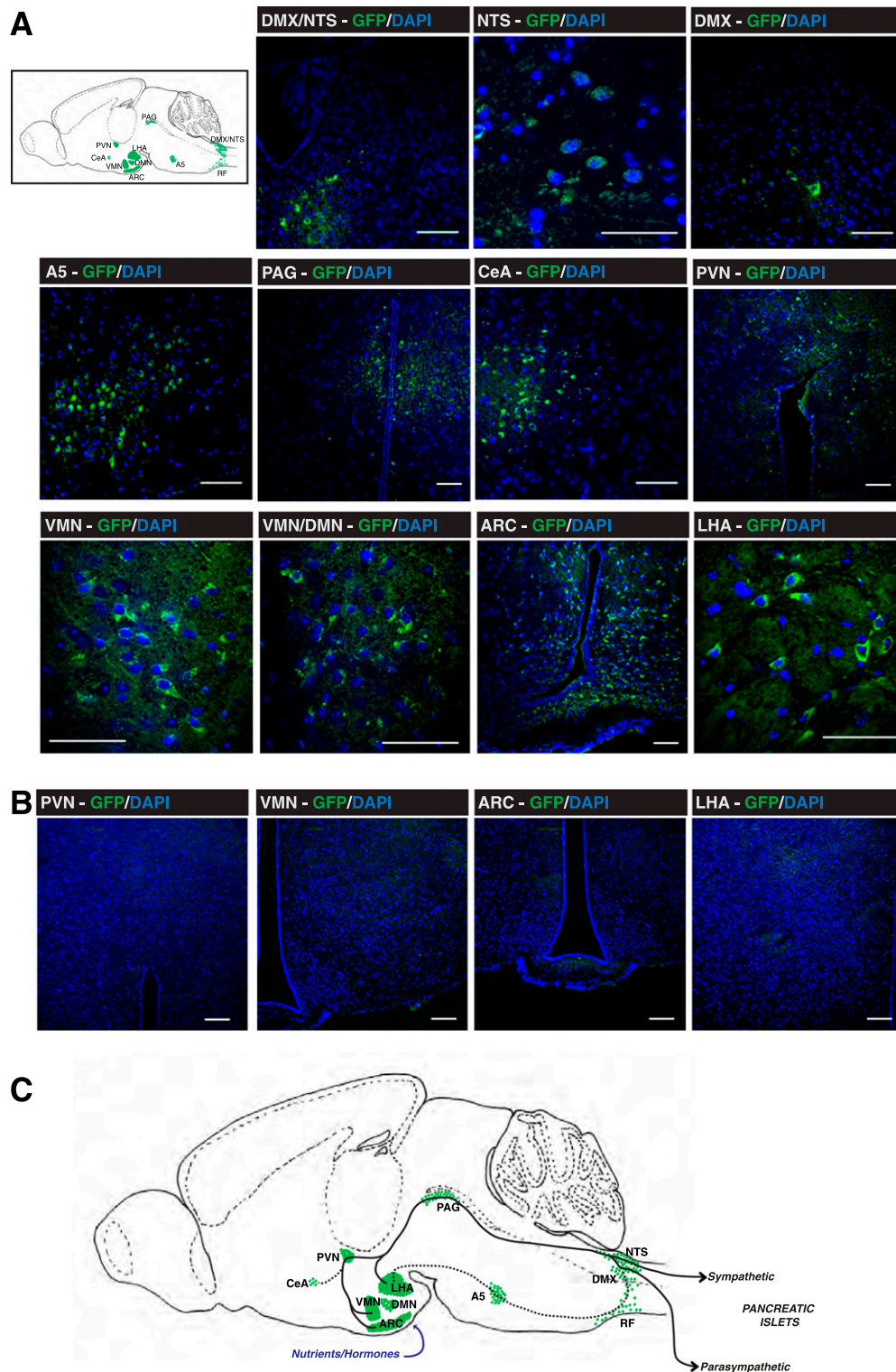
Figure 4—Brain PRV-Ba2001 tracing by β-cell–specific activation in MIP-Cre[ERT] mice. Pancreata of MIP-Cre[ERT] mice, treated either with tamoxifen (to activate nuclear Cre-recombinase specifically in pancreatic β-cells [25]) or water vehicle as a control, were infected with PRV-Ba2001, and brains were subsequently analyzed for PRV-Ba2001 retrograde neuronal migration 120 h later, as described in RESEARCH DESIGN AND METHODS. A: GFP expression (green) derived from β-cell–activated PRV-Ba2001 was detected in brain stem neuronal cells of the NTS and DMX regions; the PAG, CeA, and A5 regions; and the PVN, VMN, ARC, and LHA regions of the hypothalamus of tamoxifen-treated MIP-Cre[ERT] mice. A sagittal cartoon of the mouse brain to orient these regions is shown together with example images. The presented micrographs are from coronal sections. DAPI nuclear staining of neuronal cells is in blue. Scale bars, 50 μm. B: No PRV-Ba2001–derived GFP expression was found in hypothalamic regions of vehicle-treated MIP-Cre[ERT] control mice. C: A schematic representation of a brain-to-islet neuronal map derived from the data in Figs. 1–4. DMN, dorsomedial nucleus.
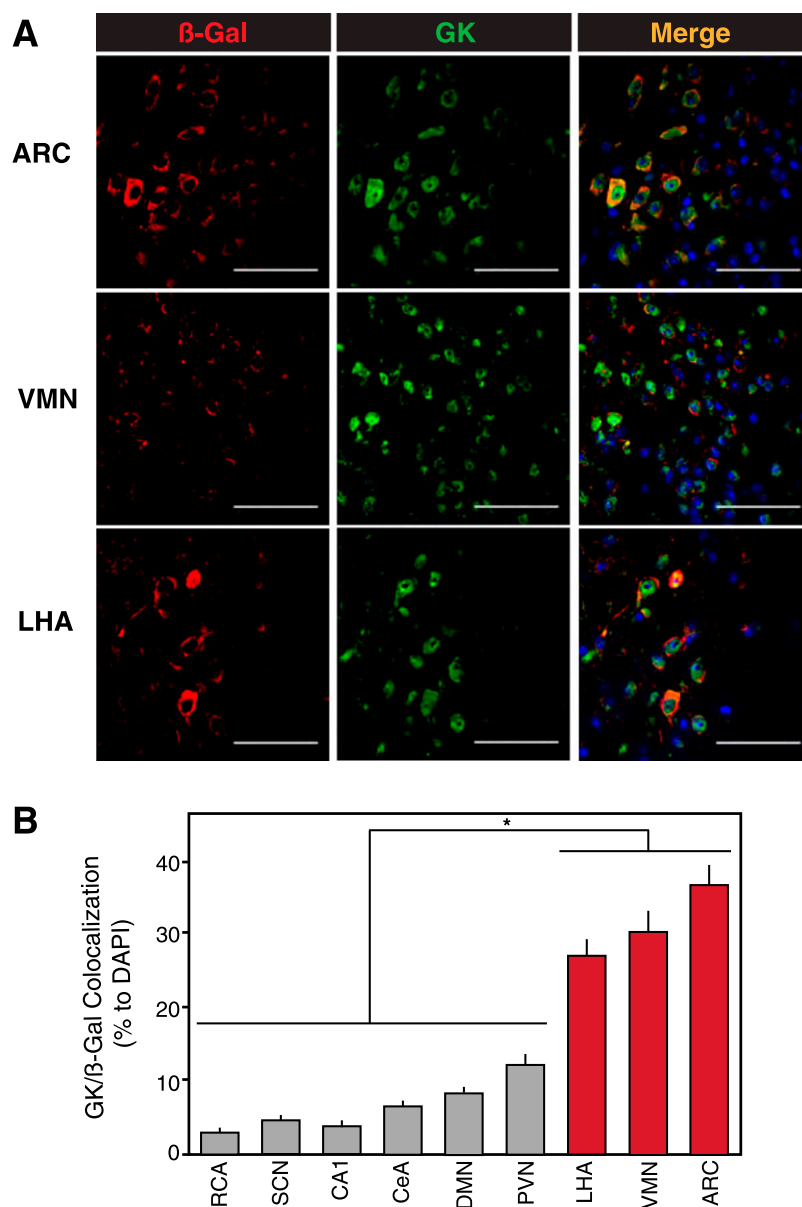
Figure 5—GK expression in the brain-to-islet map. Mice pancreata were infected with PRV-BaBlu, and 96 h later brains were analyzed for PRV-BaBlu–derived β-gal and GK expression, as described in RESEARCH DESIGN AND METHODS. *A*: Representative immunofluorescence detection of β-gal (red), GK (green), and nuclear DAPI (blue) for the ARC, VMN, and LHA regions of the hypothalamus. Scale bars, 50 μm. *B*: A quantification of β-gal/GK coexpressing neuronal cells in regions of the brain. The β-gal/GK colocalization was significantly higher in LHA, VMN, and ARC regions of the hypothalamus (red bars; $P \leq 0.001$ vs. other brain regions). Data are presented as the mean ± SEM ($n \geq 5$). DMN, dorsomedial nucleus; RCA, retrochiasmatic area.

shorter 5-h fasting glucose levels or the rebound in glucose levels in the counter-regulatory response (60–180 min) (Fig. 7*A*–*C*). Fasting glucagon levels were equivalent in ARC-targeted HK1 overexpressing to control animals (Fig. 7*F*), and the excursion in in vivo glucagon secretion during the ITT was not particularly affected relative to control animals (Fig. 7*D* and *E*). Mice with VMN-targeted HK1 overexpression also showed no change in insulin sensitivity, 5-h fasting glucose levels, or the rate of returning glucose levels to normal in the counter-regulatory response (Fig. 7*G*–*I*). But, their fasting glucagon levels were

moderately decreased compared with those of AdV-fLuc and sham controls by ~20%, ($P \leq 0.05$) (Fig. 7*K*), although the excursion in glucagon levels during the ITT was unchanged relative to control animals (Fig. 7*J* and *L*). Mice with LHA-targeted HK1 overexpression had similar 5-h fasting blood glucose levels and insulin sensitivity relative to control animals (Fig. 7*M* and *N*). The apparent steeper downward decline in glucose in the ITT results for mice with LHA-targeted HK1 overexpression appeared to indicate an improvement in insulin sensitivity and/or be reflective of a decreased glucose sensing of the threshold for
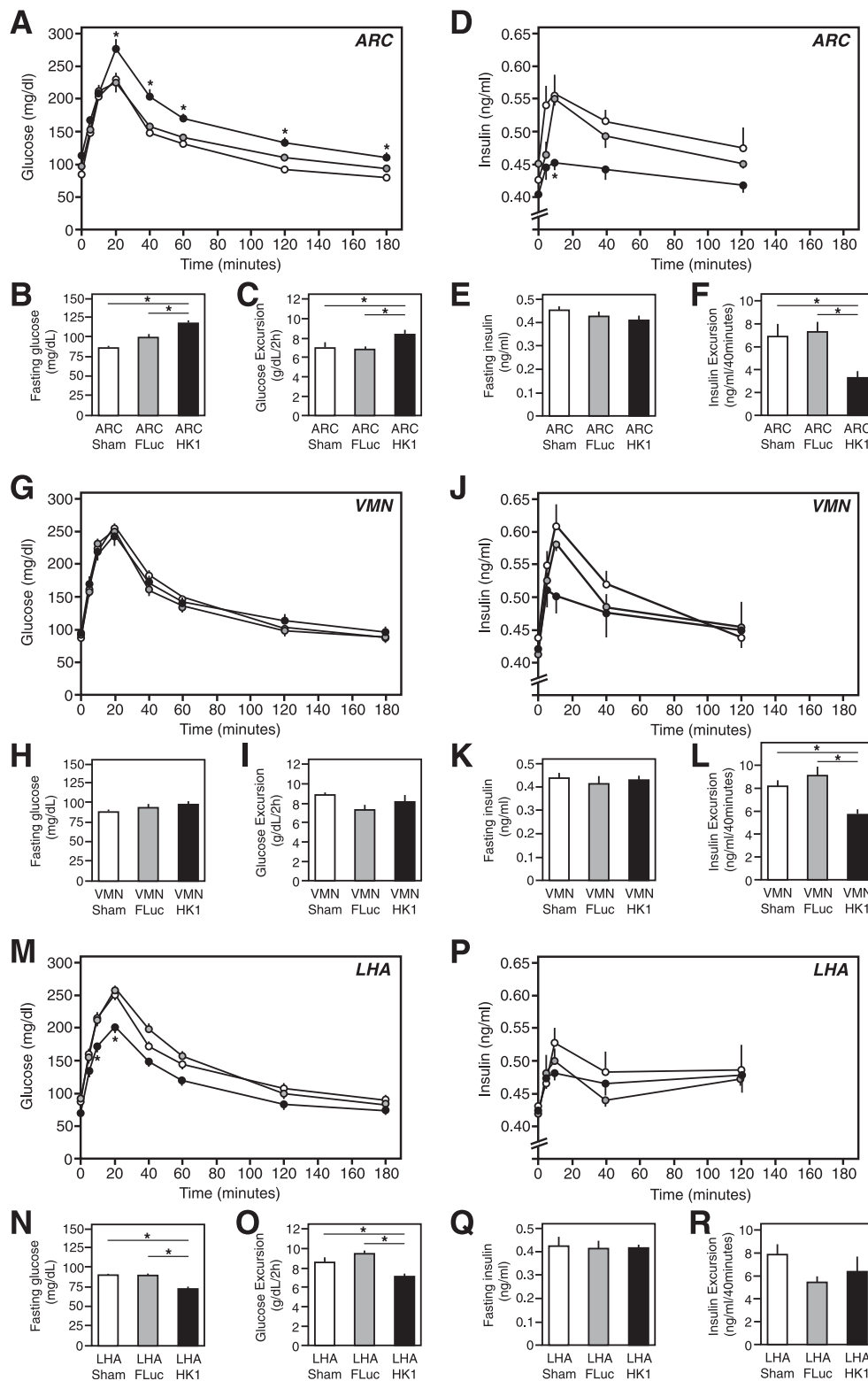
Figure 6—GTTs in mice with increased HK1 expression in the ARC, VMN, or LHA. Normal mice were subjected to stereotaxic-guided delivery of AdV-HK1, AdV-fLuc (control), or saline (sham control), specifically to the ARC, VMN, or LHA, to specifically lower glucose sensing in those brain regions, and then were subjected to a GTT, as described in RESEARCH DESIGN AND METHODS. The data are presented as the mean ± SEM ($n \geq 8$) where * indicates a statistically significant difference ($P \leq 0.05$). A, G, and M: Blood glucose levels during the GTT in the ARC, VMN, and LHA respectively. B, H, and N: Overnight fasting blood glucose levels in the ARC, VMN, and LHA, respectively. C, I, and O: Glucose excursion during the first 120 min of the GTT in the ARC, VMN, and LHA, respectively. D, J, and P: Blood insulin levels during the GTT in the ARC, VMN, and LHA, respectively. E, K, and Q: Overnight fasting blood insulin levels in the ARC, VMN, and LHA, respectively. F, L, and R: Excursion in insulin levels during the first 120 min of the GTT in the ARC, VMN, and LHA, respectively.
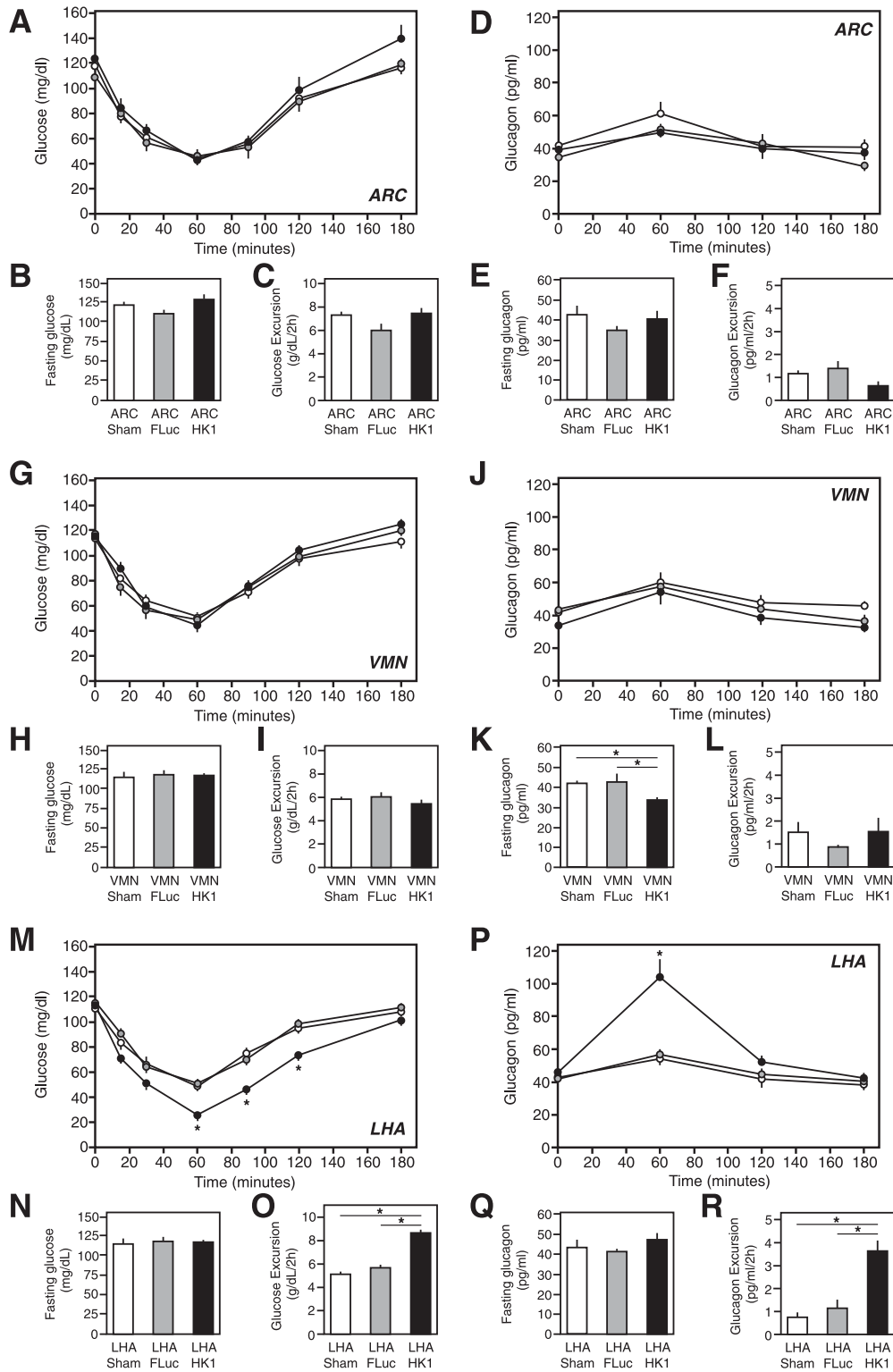
Figure 7—ITTs in mice with increased HK1 expression in the ARC, VMN, or LHA. Normal mice were subjected to stereotaxic-guided delivery of AdV-HK1, AdV-fLuc (control), or saline (sham control), specifically to the ARC, VMN, or LHA, to specifically lower glucose sensing in those brain regions, and then were subjected to an ITT, as described in RESEARCH DESIGN AND METHODS. The data are presented as the mean ± SEM ($n \geq 8$), where * indicates a statistically significant difference ($P \leq 0.05$). A, G, and M: Blood glucose levels during the ITT in the ARC, VMN, and LHA, respectively. B, H, and N: The 5-h fasting blood glucose levels in the ARC, VMN, and LHA, respectively. C, I, and O: Glucose excursion during the first 120 min of the ITT in the ARC, VMN, and LHA, respectively. D, J, and P: Blood glucagon levels during the ITT in the ARC, VMN, and LHA, respectively. E, K, and Q: Overnight fasting blood glucagon levels in the ARC, VMN, and LHA, respectively. F, L, and R: Excursion in glucagon levels during the first 120 min of the ITT in the ARC, VMN, and LHA, respectively.

counter-regulation. In control animals during the ITT, blood glucose levels went down to ~50 mg/dL at 60 min before a normal counter-regulatory response to return glucose levels to normal was observed (Fig. 7M). However, in mice with LHA-targeted HK1 overexpression, the glucose threshold for such a counter-regulatory response at 60 min was significantly reduced to a much lower 27 mg/dL ($P \leq$ 0.01) (Fig. 7M). This resulted in a greater excursion of glucose during the ITT in these animals relative to controls ($P \leq$ 0.01) (Fig. 5O), before the glucose levels returned to normal (Fig. 7M). Correspondingly, there was greater in vivo release of glucagon for this counter-regulatory response, a twofold to threefold increase over the AdV-fLuc and sham control animals ($P \leq$ 0.01) (Fig. 7P and R), without alteration in fasting glucagon levels (Fig. 7Q).

The general metabolic homeostasis was not affected by any of these manipulations, as assessed in metabolic cages. No significant differences were found in VO_2, VCO_2, respiratory exchange ratio, energy expenditure, locomotive activity, and food and water consumption between mice overexpressing HK1 in the ARC, VMN, or LHA and the equivalent fLuc-expressing and sham control mice (Supplementary Figs. 4–6). Along with a lack of effect in insulin sensitivity (Fig. 7), these data support the notion that the specific stereotaxic perturbations of glucose sensing in these distinct hypothalamic target sites drive direct short-term effects on endocrine pancreatic islet function, and are unlikely to be a consequence of affecting metabolic homeostasis to which islet α- or β-cells react secondarily.

DISCUSSION

The brain has supplementary control over pancreatic islet physiology, particularly in vivo insulin secretion from β-cells and glucagon secretion from α-cells (3,4), but the regions of the brain that mediate this regulation have been relatively undefined. Here, a newer generation of PRV recombinants has revealed a more complete map of the neuronal network specifically linking to endocrine pancreatic islets. A time course of the spread of β-gal–expressing PRV-BaBlu highlighted a major retrograde route from the pancreas to the brain stem NTS and DMX regions that, via the PAG or RF and A5 regions, reached a cul-de-sac in the PVN, ARC, VMN, and LHA in the hypothalamus. The cerebellum, SCN, CeA, and MeHab were also marked by the PRV-BaBlu infection, but the complementary use of PRV-Ba2001 in tamoxifen-treated MIP-Cre[ERT] mice marked the same regions of the brain, with the exception of the cerebellum, SCN, and MeHab. We conclude that these latter brain regions likely communicate with the exocrine or ductal pancreas and are not part of the brain-to-islet map. Thus, collectively these retrograde PRV tracing studies suggest that circulating nutrients and/or certain hormones are sensed at the base of the hypothalamus, an interoceptive center that integrates a variety of parameters crucial to maintaining homeostasis (40), and is where the ARC, VMN, and LHA reside. Neurons in these regions then communicate alongside the

third ventricle to the PVN, through the PAG to the DMX and NTS nuclei in the brain stem. Because the LHA was marked in the time course of retrograde PRV tracing, prior to the ARC and VMN, it may also have a direct route to the brain stem via A5 and RF regions, bypassing the PVN and PAG (Fig. 4C).

This brain-to-islet map builds on the findings of previous studies (22,23), and is known to contain both parasympathetic and sympathetic neuronal circuits. The brain regions that link to pancreatic islet cells are identified by this map and make sense. The DMX is the dorsal motor nucleus of the vagus nerve (indeed the vagus is known to link to the endocrine pancreas (19,20), and the NTS contains a concentration of neurons that connects with the PVN of the hypothalamus and the gastrointestinal tract (41,42). The ARC and VMN are well known for the regulation of satiety, metabolic homeostasis, and hypoglycemic counter-regulation responses, especially the control of glucose release, among other functions (43–46). The LHA is an orexigenic center involved in appetite, wakefulness, and energy expenditure (47). As such, it is intuitive that specific neuronal circuitry within these regions may also have a direct influence on pancreatic islet physiology, especially the secretion of insulin and glucagon.

Hypothalamic glucose sensing may have a degree of control over pancreatic islet hormone secretion (21,48). Here, GK-expressing neurons were most commonly found in the brain-to-islet neuronal network map of ARC, VMN, and LHA. Whereas GK expression in the brain is not a new finding, its overlap with endocrine pancreas–projecting neurons is novel. In order to render some functional validation to this map, as well as to gain insight into centrally mediated control of pancreatic islet function, glucose sensing was altered by selective HK1 overexpression in the ARC, VMN, and LHA. Again, it is emphasized that this manipulation was conducted primarily to see whether the same alteration in glucose-sensing hypothalamic regions within the brain-to-islet map had direct effects on islet cell functions, and any insight into the regulation of glucose homeostasis should be considered secondarily and preliminary, requiring additional experimentation to substantiate these initial findings. Nonetheless, we found distinct effects on insulin and glucagon secretion, depending on the hypothalamic region manipulated. Increased HK1 expression in the ARC rendered the animals glucose intolerant because of reduced glucose-induced insulin secretion. This complemented studies using intracerebroventricular administration of GK inhibitors (49), but here we specifically localized this effect to the ARC. In contrast, HK1 overexpression in the VMN did not affect glucose tolerance despite a modest reduction in glucose-induced insulin secretion, and the counter-regulatory response to hypoglycemia was normal despite glucagon secretion being slightly reduced. Studies (43,44) have implicated the VMN in hypoglycemic counter-regulation via regulation of glucagon and epinephrine responses. However, the inhibition of VMN GK using stereotaxic AdV-mediated delivery of GK

short hairpin RNA, perhaps complementary to VMN-targeted HK1 overexpression in this study, also had no significant effect on glucagon and epinephrine during an ITT counter-regulatory response (50). Nonetheless, it should be noted that the VMN is a much larger area to target than the ARC, and it is possible that not all of this area was subjected to increased HK1 expression that may dampen an effect. In the same vein, it is possible that some HK1 targeted to the larger VMN leaked over into the ARC, rendering a slight blunting of glucose-induced insulin secretion. However, it is also likely that insulin signaling in the VMN triggers a counter-regulatory response to increase glucagon secretion (51). GK-expressing neurons of the brain-to-islet map were also in the LHA. Intriguingly, HK1 overexpression specifically in the LHA appeared to alter the threshold for glucose tolerance and hypoglycemic counter-regulatory responses. An apparent improved glucose tolerance could be due to lowering the set point for glucose sensing, where the overnight fasting glucose level was significantly lower, which in turn reduced the excursion in glucose levels in the GTT without affecting insulin secretion. The effect of lowering the threshold for glucose sensing was more pronounced in a counter-regulatory response to hypoglycemia in an ITT that provoked a markedly increased glucagon response. However, these data could also be interpreted that HK1 overexpression in the LHA might also result in improved insulin sensitivity. As such, further experimentation will be necessary in future studies to indicate whether this is due to a lowering of the threshold for glucose metabolic homeostasis and counter-regulatory glucagon responses (e.g., hypoglycemic clamp studies) and/or increased insulin sensitivity (e.g., hyperinsulinemic-euglycemic clamp studies). Nonetheless, implicating the LHA in setting metabolic thresholds that directly affect pancreatic islet hormone secretion is a novel observation and may have implications for the treatment of obesity-linked type 2 diabetes. In obese Zucker diabetic rats, where there are increased insulin and reduced glucagon levels relative to those of lean control rats (52), there is an increased threshold for local LHA dopamine release relative to that of lean controls (53). If alteration of the glucose threshold in the LHA can be linked to local dopaminergic responses, then this could be, in part, the basis of current novel therapeutic approaches to treat type 2 diabetes using dopamine agonists (54).

Collectively, these observations show that the brain-to-islet map is functional. They also underline the complexity of CNS control of pancreatic islet function. Although each hypothalamic region has a different effect on insulin and/or glucagon secretion, they undoubtedly coordinate with each other to give a coordinated response (48), as would glucose-excitable and glucose-inhibited neurons (55). Glucose sensing in the ARC appears to directly regulate insulin secretion, which is in synchrony with the LHA to set glucose-sensing thresholds and/or alter insulin sensitivity that then supplements the regulation of glucagon secretion.

This contributes to an overall coordinated central control for tightly maintaining general glucose homeostasis (48). Although this study unveils the most detailed functional brain-to-islet neuronal map to date, further experimentation will be needed to refine it and gain a better specification for the neuronal circuits within. Moreover, there are unquestionably other factors (e.g., other nutrients, hormones, and neurotransmitters) that could also trigger specific circuits within this map in coordination with glucose-regulated circuits. Because of such complexity, this brain-to-islet map is best considered as a guiding draft for future studies that will be continually added to for further refinement, and eventually may lead to novel targeted therapies to treat obesity and/or type 2 diabetes.

Author Contributions. W.R. conceived and designed the project; provided, generated, and/or purified viral vector preparations; conducted PRV tracing surgery and stereotaxic surgery; conducted tissue preparation, image acquisition and analysis, all other metabolic assessments, and data analysis and interpretation; and wrote and edited the manuscript. I.S. conducted PRV tracing surgery, tissue preparation, and image acquisition and analysis. A.W. conducted tissue preparation and image acquisition and analysis. C.P. conducted PRV tracing surgery. J.F. conducted stereotaxic surgery. T.C.B. provided, generated, and/or purified viral vector preparations and generated the adenovirus-HK1 vector. A.A. and L.W.E. provided, generated, and/or purified viral vector preparations. N.T. and L.H.P. originally provided MIP-Cre[ERT] mice. M.G.M. conceived and designed the project. C.J.R. conceived and designed the project, conducted data analysis and interpretation, and wrote and edited the manuscript. C.J.R. is the guarantor of this work and, as such, had full access to all the data in the study and takes responsibility for the integrity of the data and the accuracy of the data analysis.

References

1. Gerich JE, Charles MA, Grodsky GM. Regulation of pancreatic insulin and glucagon secretion. Annu Rev Physiol 1976;38:353–388

2. Unger RH, Dobbs RE, Orci L. Insulin, glucagon, and somatostatin secretion in the regulation of metabolism. Annu Rev Physiol 1978;40:307–343

3. Porte D Jr, Smith PH, Ensinck JW. Neurohumoral regulation of the pancreatic islet A and B cells. Metabolism 1976;25(Suppl. 1):1453–1456

4. Dunning BE, Taborsky GJJ Jr. Neural control of islet function by norepinephrine and sympathetic neuropeptides. Adv Exp Med Biol 1991;291:107–127

5. Bernard C. Influence de la section des pédoncules cérébelleux moyens sur la composition de l'urine. C R Soc Biol 1849;1:14–18 [in French]

6. Bloom SR, Edwards AV. The release of pancreatic glucagon and inhibition of insulin in response to stimulation of the sympathetic innervation. J Physiol 1975; 253:157–173

7. Ahrén B, Taborsky GJJ Jr. The mechanism of vagal nerve stimulation of glucagon and insulin secretion in the dog. Endocrinology 1986;118:1551–1557

8. Frohman LA, Ezdinli EZ, Javid R. Effect of vagotomy and vagal stimulation on insulin secretion. Diabetes 1967;16:443–448

9. Bloom SR, Edwards AV, Vaughan NJA. The role of the autonomic innervation in the control of glucagon release during hypoglycaemia in the calf. J Physiol 1974;236:611–623

10. Humphrey CS, Dykes JR, Johnston D. Effects of truncal, selective, and highly selective vagotomy on glucose tolerance and insulin secretion in patients with duodenal ulcer. Part I-Effect of vagotomy on response to oral glucose. BMJ 1975;2:112–114

11. Heinzen BR. Observations on the innervation of the pancreatic islets. Arch Surg 1960;81:627–631

12. Bloom SR. Blood glucose control by direct islet innervation. Horm Metab Res 1976;(Suppl. 6):85–90

13. Gregg BE, Moore PC, Demozay D, et al. Formation of a human β-cell population within pancreatic islets is set early in life. J Clin Endocrinol Metab 2012;97:3197–3206

14. Rodriguez-Diaz R, Abdulreda MH, Formoso AL, et al. Innervation patterns of autonomic axons in the human endocrine pancreas. Cell Metab 2011;14:45–54

15. Taborsky GJJ Jr. Islets have a lot of nerve! Or do they? Cell Metab 2011;14: 5–6

16. Sorenson RL, Elde RP, Seybold V. Effect of norepinephrine on insulin, glucagon, and somatostatin secretion in isolated perifused rat islets. Diabetes 1979;28:899–904

17. Yajima H, Komatsu M, Sato Y, et al. Norepinephrine inhibits glucose-stimulated, Ca2+-independent insulin release independently from its action on adenylyl cyclase. Endocr J 2001;48:647–654

18. Duttaroy A, Zimliki CL, Gautam D, Cui Y, Mears D, Wess J. Muscarinic stimulation of pancreatic insulin and glucagon release is abolished in m3 muscarinic acetylcholine receptor-deficient mice. Diabetes 2004;53:1714–1720

19. Imai J, Katagiri H, Yamada T, et al. Regulation of pancreatic beta cell mass by neuronal signals from the liver. Science 2008;322:1250–1254

20. Lausier J, Diaz WC, Roskens V, et al. Vagal control of pancreatic ß-cell proliferation. Am J Physiol Endocrinol Metab 2010;299:E786–E793

21. Osundiji MA, Evans ML. Brain control of insulin and glucagon secretion. Endocrinol Metab Clin North Am 2013;42:1–14

22. Jansen AS, Hoffman JL, Loewy AD. CNS sites involved in sympathetic and parasympathetic control of the pancreas: a viral tracing study. Brain Res 1997; 766:29–38

23. Buijs RM, Chun SJ, Niijima A, Romijn HJ, Nagai K. Parasympathetic and sympathetic control of the pancreas: a role for the suprachiasmatic nucleus and other hypothalamic centers that are involved in the regulation of food intake. J Comp Neurol 2001;431:405–423

24. Tokunaga K, Fukushima M, Kemnitz JW, Bray GA. Effect of vagotomy on serum insulin in rats with paraventricular or ventromedial hypothalamic lesions. Endocrinology 1986;119:1708–1711

25. Wicksteed B, Brissova M, Yan W, et al. Conditional gene targeting in mouse pancreatic ß-Cells: analysis of ectopic Cre transgene expression in the brain. Diabetes 2010;59:3090–3098

26. Yaekura K, Julyan R, Wicksteed BL, et al. Insulin secretory deficiency and glucose intolerance in Rab3A null mice. J Biol Chem 2003;278:9715–9721

27. Franklin KBJ, Paxinos G. *The Mouse Brain in Stereotaxic Coordinates*. Amsterdam, Elsevier/Academic Press, 2008

28. Card JP, Enquist LW. Transneuronal circuit analysis with pseudorabies viruses. Curr Protoc Neurosci 2014;68:1.5.1–1.5.39

29. Wrede CE, Dickson LM, Lingohr MK, Briaud I, Rhodes CJ. Protein kinase B/Akt prevents fatty acid-induced apoptosis in pancreatic beta-cells (INS-1). J Biol Chem 2002;277:49676–49684

30. Flak JN, Patterson CM, Garfield AS, et al. Leptin-inhibited PBN neurons enhance counter-regulatory responses to hypoglycemia in negative energy balance. Nat Neurosci 2014;17:1744–1750

31. Enquist LW, Card JP. Recent advances in the use of neurotropic viruses for circuit analysis. Curr Opin Neurobiol 2003;13:603–606

32. DeFalco J, Tomishima M, Liu H, et al. Virus-assisted mapping of neural inputs to a feeding center in the hypothalamus. Science 2001;291:2608–2613

33. Smith EP, An Z, Wagner C, et al. The role of β cell glucagon-like peptide-1 signaling in glucose regulation and response to diabetes drugs. Cell Metab 2014; 19:1050–1057

34. Jetton TL, Liang Y, Pettepher CC, et al. Analysis of upstream glucokinase promoter activity in transgenic mice and identification of glucokinase in rare neuroendocrine cells in the brain and gut. J Biol Chem 1994;269:3641–3654

35. Yang XJ, Kow LM, Funabashi T, Mobbs CV. Hypothalamic glucose sensor: similarities to and differences from pancreatic beta-cell mechanisms. Diabetes 1999;48:1763–1772

36. Iynedjian PB. Molecular physiology of mammalian glucokinase. Cell Mol Life Sci 2009;66:27–42

37. Wilson JE. Hexokinases. Rev Physiol Biochem Pharmacol 1995;126:65–198

38. Becker TC, BeltrandelRio H, Noel RJ, Johnson JH, Newgard CB. Over-expression of hexokinase I in isolated islets of Langerhans via recombinant adenovirus. Enhancement of glucose metabolism and insulin secretion at basal but not stimulatory glucose levels. J Biol Chem 1994;269:21234–21238

39. Morton GJ, Niswender KD, Rhodes CJ, et al. Arcuate nucleus-specific leptin receptor gene therapy attenuates the obesity phenotype of Koletsky (fa(k)/fa(k)) rats. Endocrinology 2003;144:2016–2024

40. Saper CB, Lowell BB. The hypothalamus. Curr Biol 2014;24:R1111–R1116

41. Valassi E, Scacchi M, Cavagnini F. Neuroendocrine control of food intake. Nutr Metab Cardiovasc Dis 2008;18:158–168

42. Konturek SJ, Konturek JW, Pawlik T, Brzozowski T. Brain-gut axis and its role in the control of food intake. J Physiol Pharmacol 2004;55:137–154

43. Borg WP, During MJ, Sherwin RS, Borg MA, Brines ML, Shulman GI. Ventromedial hypothalamic lesions in rats suppress counterregulatory responses to hypoglycemia. J Clin Invest 1994;93:1677–1682

44. Borg WP, Sherwin RS, During MJ, Borg MA, Shulman GI. Local ventromedial hypothalamus glucopenia triggers counterregulatory hormone release. Diabetes 1995;44:180–184

45. Morton GJ, Schwartz MW. Leptin and the central nervous system control of glucose metabolism. Physiol Rev 2011;91:389–411

46. Könner AC, Klöckener T, Brüning JC. Control of energy homeostasis by insulin and leptin: targeting the arcuate nucleus and beyond. Physiol Behav 2009; 97:632–638

47. Burt J, Alberto CO, Parsons MP, Hirasawa M. Local network regulation of orexin neurons in the lateral hypothalamus. Am J Physiol Regul Integr Comp Physiol 2011;301:R572–R580

48. Schwartz MW, Seeley RJ, Tschöp MH, et al. Cooperation between brain and islet in glucose homeostasis and diabetes. Nature 2013;503:59–66

49. Osundiji MA, Lam DD, Shaw J, et al. Brain glucose sensors play a significant role in the regulation of pancreatic glucose-stimulated insulin secretion. Diabetes 2012;61:321–328

50. Levin BE, Becker TC, Eiki J, Zhang BB, Dunn-Meynell AA. Ventromedial hypothalamic glucokinase is an important mediator of the counterregulatory response to insulin-induced hypoglycemia. Diabetes 2008;57:1371–1379

51. Fisher SJ, Brüning JC, Lannon S, Kahn CR. Insulin signaling in the central nervous system is critical for the normal sympathoadrenal response to hypoglycemia. Diabetes 2005;54:1447–1451

52. Bray GA. The Zucker-fatty rat: a review. Fed Proc 1977;36:148–153

53. Yang ZJ, Meguid MM. LHA dopaminergic activity in obese and lean Zucker rats. Neuroreport 1995;6:1191–1194

54. Defronzo RA. Bromocriptine: a sympatholytic, d2-dopamine agonist for the treatment of type 2 diabetes. Diabetes Care 2011;34:789–794

55. Ogunnowo-Bada EO, Heeley N, Brochard L, Evans ML. Brain glucose sensing, glucokinase and neural control of metabolism and islet function. Diabetes Obes Metab 2014;16(Suppl. 1):26–32